The Astrophysical Journal, 988:141 (15pp), 2025 July 20 https://doi.org/10.3847/1538-4357/addd05

IceCube Search for Neutrino Emission from X-Ray Bright Seyfert Galaxies

R. Abbasi[1], M. Ackermann[2], J. Adams[3], S. K. Agarwalla[4,68], J. A. Aguilar[5], M. Ahlers[6], J. M. Alameddine[7], N. M. Amin[8], K. Andeen[9], C. Argüelles[10], Y. Ashida[11], S. Athanasiadou[2], L. Ausborn[12], S. N. Axani[8], X. Bai[13], A. Balagopal V.[4], M. Baricevic[4], S. W. Barwick[14], S. Bash[15], V. Basu[4], R. Bay[16], J. J. Beatty[17,18], J. Becker Tjus[19,69], J. Beise[20], C. Bellenghi[15], C. Benning[12], S. BenZvi[21], D. Berley[22], E. Bernardini[23], D. Z. Besson[24], E. Blaufuss[22], L. Bloom[25], S. Blot[2], F. Bontempo[26], J. Y. Book Motzkin[10], C. Boscolo Meneguolo[23], S. Böser[27], O. Botner[20], J. Böttcher[12], J. Braun[4], B. Brinson[28], J. Brostean-Kaiser[2], L. Brusa[12], R. T. Burley[29], D. Butterfield[4], M. A. Campana[30], I. Caracas[27], K. Carloni[10], J. Carpio[31,32], S. Chattopadhyay[4,68], N. Chau[5], Z. Chen[33], D. Chirkin[4], S. Choi[34,35], B. A. Clark[22], A. Coleman[20], G. H. Collin[36], A. Connolly[17,18], J. M. Conrad[36], P. Coppin[37], R. Corley[11], P. Correa[37], D. F. Cowen[38,39], P. Dave[28], C. De Clercq[37], J. J. DeLaunay[25], D. Delgado[10], S. Deng[12], A. Desai[4], P. Desiati[4], K. D. de Vries[37], G. de Wasseige[40], T. DeYoung[41], A. Diaz[36], J. C. Díaz-Vélez[4], P. Dierichs[12], M. Dittmer[42], A. Domi[43], L. Draper[11], H. Dujmovic[4], K. Dutta[27], M. A. DuVernois[4], T. Ehrhardt[27], L. Eidenschink[15], A. Eimer[43], P. Eller[15], E. Ellinger[44], S. El Mentawi[12], D. Elsässer[7], R. Engel[26,45], H. Erpenbeck[4], J. Evans[22], P. A. Evenson[8], K. L. Fan[22], K. Fang[4], K. Farrag[46], A. R. Fazely[47], A. Fedynitch[48], N. Feigl[49], S. Fiedlschuster[43], C. Finley[50], L. Fischer[2], D. Fox[38], A. Franckowiak[19], S. Fukami[2], P. Fürst[12], J. Gallagher[51], E. Ganster[12], A. Garcia[10], M. Garcia[8], G. Garg[4,68], E. Genton[10,40], L. Gerhardt[52], A. Ghadimi[25], C. Girard-Carillo[27], C. Glaser[20], T. Glauch[15], T. Glüsenkamp[20,43], J. G. Gonzalez[8], S. Goswami[31,32], A. Granados[41], D. Grant[41], S. J. Gray[22], O. Gries[12], S. Griffin[4], S. Griswold[21], K. M. Groth[6], C. Günther[12], P. Gutjahr[7], C. Ha[53], C. Haack[43], A. Hallgren[20], L. Halve[12], F. Halzen[4], H. Hamdaoui[33], M. Ha Minh[15], M. Handt[12], K. Hanson[4], J. Hardin[36], A. A. Harnisch[41], P. Hatch[54], A. Haungs[26], J. Häussler[12], K. Helbing[44], J. Hellrung[19], J. Hermannsgabner[12], L. Heuermann[12], N. Heyer[20], S. Hickford[44], A. Hidvegi[50], C. Hill[46], G. C. Hill[29], K. D. Hoffman[22], S. Hori[4], K. Hoshina[4,70], M. Hostert[10], W. Hou[26], T. Huber[26], K. Hultqvist[50], M. Hünnefeld[7], R. Hussain[4], K. Hymon[7], A. Ishihara[46], W. Iwakiri[46], M. Jacquart[4], O. Janik[43], M. Jansson[50], G. S. Japaridze[55], M. Jeong[11], M. Jin[10], B. J. P. Jones[56], N. Kamp[10], D. Kang[26], W. Kang[34], X. Kang[30], A. Kappes[42], D. Kappesser[27], L. Kardum[7], T. Karg[2], M. Karl[15], A. Karle[4], A. Katil[57], U. Katz[43], M. Kauer[4], J. L. Kelley[4], M. Khanal[11], A. Khatee Zathul[4], A. Kheirandish[31,32], J. Kiryluk[33], S. R. Klein[16,52], A. Kochocki[41], R. Koirala[8], H. Kolanoski[49], T. Kontrimas[15], L. Köpke[27], C. Kopper[43], D. J. Koskinen[6], P. Koundal[8], M. Kovacevich[30], M. Kowalski[2,49], T. Kozynets[6], J. Krishnamoorthi[4,68], K. Kruiswijk[40], E. Krupczak[41], A. Kumar[2], E. Kun[19], N. Kurahashi[30], N. Lad[2], C. Lagunas Gualda[2], M. Lamoureux[40], M. J. Larson[22], S. Latseva[12], F. Lauber[44], J. P. Lazar[40], J. W. Lee[34], K. Leonard DeHolton[39], A. Leszczyńska[8], J. Liao[28], M. Lincetto[19], Q. R. Liu[54,58,59], Y. T. Liu[39], M. Liubarska[57], E. Lohfink[27], C. Love[30], C. J. Lozano Mariscal[42], L. Lu[4], F. Lucarelli[60], W. Luszczak[17,18], Y. Lyu[16,52], J. Madsen[4], E. Magnus[37], K. B. M. Mahn[41], Y. Makino[4], E. Manao[15], S. Mancina[4,23], W. Marie Sainte[4], I. C. Mariş[5], S. Marka[61], Z. Marka[61], M. Marsee[25], I. Martinez-Soler[10], R. Maruyama[62], F. Mayhew[41], F. McNally[63], J. V. Mead[6], K. Meagher[4], S. Mechbal[2], A. Medina[18], M. Meier[46], Y. Merckx[37], L. Merten[19], J. Micallef[41], J. Mitchell[47], T. Montaruli[60], R. W. Moore[57], Y. Morii[46], R. Morse[4], M. Moulai[4], T. Mukherjee[26], R. Naab[2], R. Nagai[46], M. Nakos[4], U. Naumann[44], J. Necker[2], A. Negi[56], L. Neste[50], M. Neumann[42], H. Niederhausen[41], M. U. Nisa[41], K. Noda[46], A. Noell[12], A. Novikov[8], A. Obertacke Pollmann[46], V. O'Dell[4], B. Oeyen[64], A. Olivas[22], R. Orsoe[15], J. Osborn[4], E. O'Sullivan[20], H. Pandya[8], N. Park[54], G. K. Parker[56], E. N. Paudel[8], L. Paul[13], C. Pérez de los Heros[20], T. Pernice[2], J. Peterson[4], S. Philippen[12], A. Pizzuto[4], M. Plum[13], A. Pontén[20], Y. Popovych[27], M. Prado Rodriguez[4], B. Pries[41], R. Procter-Murphy[22], G. T. Przybylski[52], C. Raab[40], J. Rack-Helleis[27], M. Ravn[20], K. Rawlins[65], Z. Rechav[4], A. Rehman[8], P. Reichherzer[19], E. Resconi[15], S. Reusch[2], W. Rhode[7], B. Riedel[4], A. Rifaie[12], E. J. Roberts[29], S. Robertson[16,52], S. Rodan[34,35], G. Roellinghoff[34], M. Rongen[43], A. Rosted[46], C. Rott[11,34], T. Ruhe[7], L. Ruohan[15], D. Ryckbosch[64], I. Safa[4], J. Saffer[45], D. Salazar-Gallegos[41], P. Sampathkumar[26], A. Sandrock[44], M. Santander[25], S. Sarkar[57], S. Sarkar[66], J. Savelberg[12], P. Savina[4], P. Schaile[15], M. Schaufel[12], H. Schieler[26], S. Schindler[43], B. Schlüter[42], F. Schlüter[5], N. Schmeisser[44], T. Schmidt[22], J. Schneider[43], F. G. Schröder[8,26], L. Schumacher[43], S. Sclafani[22], D. Seckel[8], M. Seikh[24], M. Seo[34], S. Seunarine[67], P. Sevle Myhr[40], R. Shah[30], S. Shefali[45], N. Shimizu[46], M. Silva[4], B. Skrzypek[16], B. Smithers[56], R. Snihur[4], J. Soedingrekso[7], A. Søgaard[6], D. Soldin[11], P. Soldin[12], G. Sommani[19], C. Spannfellner[15], G. M. Spiczak[67], C. Spiering[2], M. Stamatikos[18], T. Stanev[8], T. Stezelberger[52], T. Stürwald[44], T. Stuttard[6], G. W. Sullivan[22], I. Taboada[28], S. Ter-Antonyan[47], A. Terliuk[15], M. Thiesmeyer[12], W. G. Thompson[10], J. Thwaites[4], S. Tilav[8], K. Tollefson[41], C. Tönnis[34], S. Toscano[5], D. Tosi[4], A. Trettin[2], R. Turcotte[26], J. P. Twagirayezu[41], M. A. Unland Elorrieta[42], A. K. Upadhyay[4,68], K. Upshaw[47], A. Vaidyanathan[9], N. Valtonen-Mattila[20], J. Vandenbroucke[4], N. van Eijndhoven[37], D. Vannerom[36], J. van Santen[2], J. Vara[42], F. Varsi[45], J. Veitch-Michaelis[4], M. Venugopal[26], M. Vereecken[40], S. Verpoest[8], D. Veske[61], A. Vijai[22], C. Walck[50], A. Wang[28], C. Weaver[41],

P. Weigel[36], A. Weindl[26], J. Weldert[39], A. Y. Wen[10], C. Wendt[4], J. Werthebach[7], M. Weyrauch[26], N. Whitehorn[41], C. H. Wiebusch[12], D. R. Williams[25], L. Witthaus[7], A. Wolf[12], M. Wolf[15], G. Wrede[43], X. W. Xu[47], J. P. Yanez[57], E. Yildizci[4], S. Yoshida[46], R. Young[24], S. Yu[11], T. Yuan[4], Z. Zhang[33], P. Zhelnin[10], P. Zilberman[4], and M. Zimmerman[4]

[1] Department of Physics, Loyola University Chicago, Chicago, IL 60660, USA; analysis@icecube.wisc.edu
[2] Deutsches Elektronen-Synchrotron DESY, Platanenallee 6, D-15738 Zeuthen, Germany
[3] Dept. of Physics and Astronomy, University of Canterbury, Private Bag 4800, Christchurch, New Zealand
[4] Dept. of Physics and Wisconsin IceCube Particle Astrophysics Center, University of Wisconsin—Madison, Madison, WI 53706, USA
[5] Université Libre de Bruxelles, Science Faculty CP230, B-1050 Brussels, Belgium
[6] Niels Bohr Institute, University of Copenhagen, DK-2100 Copenhagen, Denmark
[7] Dept. of Physics, TU Dortmund University, D-44221 Dortmund, Germany
[8] Bartol Research Institute and Dept. of Physics and Astronomy, University of Delaware, Newark, DE 19716, USA
[9] Department of Physics, Marquette University, Milwaukee, WI 53201, USA
[10] Department of Physics and Laboratory for Particle Physics and Cosmology, Harvard University, Cambridge, MA 02138, USA
[11] Department of Physics and Astronomy, University of Utah, Salt Lake City, UT 84112, USA
[12] III. Physikalisches Institut, RWTH Aachen University, D-52056 Aachen, Germany
[13] Physics Department, South Dakota School of Mines and Technology, Rapid City, SD 57701, USA
[14] Dept. of Physics and Astronomy, University of California, Irvine, CA 92697, USA
[15] Physik-department, Technische Universität München, D-85748 Garching, Germany
[16] Dept. of Physics, University of California, Berkeley, CA 94720, USA
[17] Dept. of Astronomy, Ohio State University, Columbus, OH 43210, USA
[18] Dept. of Physics and Center for Cosmology and Astro-Particle Physics, Ohio State University, Columbus, OH 43210, USA
[19] Fakultät für Physik & Astronomie, Ruhr-Universität Bochum, D-44780 Bochum, Germany
[20] Dept. of Physics and Astronomy, Uppsala University, Box 516, SE-75120 Uppsala, Sweden
[21] Dept. of Physics and Astronomy, University of Rochester, Rochester, NY 14627, USA
[22] Dept. of Physics, University of Maryland, College Park, MD 20742, USA
[23] Dipartimento di Fisica e Astronomia Galileo Galilei, Università Degli Studi di Padova, I-35122 Padova PD, Italy
[24] Dept. of Physics and Astronomy, University of Kansas, Lawrence, KS 66045, USA
[25] Dept. of Physics and Astronomy, University of Alabama, Tuscaloosa, AL 35487, USA
[26] Karlsruhe Institute of Technology, Institute for Astroparticle Physics, D-76021 Karlsruhe, Germany
[27] Institute of Physics, University of Mainz, Staudinger Weg 7, D-55099 Mainz, Germany
[28] School of Physics and Center for Relativistic Astrophysics, Georgia Institute of Technology, Atlanta, GA 30332, USA
[29] Department of Physics, University of Adelaide, Adelaide, 5005, Australia
[30] Dept. of Physics, Drexel University, 3141 Chestnut Street, Philadelphia, PA 19104, USA
[31] Department of Physics & Astronomy, University of Nevada, Las Vegas, NV 89154, USA
[32] Nevada Center for Astrophysics, University of Nevada, Las Vegas, NV 89154, USA
[33] Dept. of Physics and Astronomy, Stony Brook University, Stony Brook, NY 11794-3800, USA
[34] Dept. of Physics, Sungkyunkwan University, Suwon 16419, Republic of Korea
[35] Institute of Basic Science, Sungkyunkwan University, Suwon 16419, Republic of Korea
[36] Dept. of Physics, Massachusetts Institute of Technology, Cambridge, MA 02139, USA
[37] Vrije Universiteit Brussel (VUB), Dienst ELEM, B-1050 Brussels, Belgium
[38] Dept. of Astronomy and Astrophysics, Pennsylvania State University, University Park, PA 16802, USA
[39] Dept. of Physics, Pennsylvania State University, University Park, PA 16802, USA
[40] Centre for Cosmology, Particle Physics and Phenomenology - CP3, Université catholique de Louvain, Louvain-la-Neuve, Belgium
[41] Dept. of Physics and Astronomy, Michigan State University, East Lansing, MI 48824, USA
[42] Institut für Kernphysik, Westfälische Wilhelms-Universität Münster, D-48149 Münster, Germany
[43] Erlangen Centre for Astroparticle Physics, Friedrich-Alexander-Universität Erlangen-Nürnberg, D-91058 Erlangen, Germany
[44] Dept. of Physics, University of Wuppertal, D-42119 Wuppertal, Germany
[45] Karlsruhe Institute of Technology, Institute of Experimental Particle Physics, D-76021 Karlsruhe, Germany
[46] Dept. of Physics and The International Center for Hadron Astrophysics, Chiba University, Chiba 263-8522, Japan
[47] Dept. of Physics, Southern University, Baton Rouge, LA 70813, USA
[48] Institute of Physics, Academia Sinica, Taipei, 11529, Taiwan
[49] Institut für Physik, Humboldt-Universität zu Berlin, D-12489 Berlin, Germany
[50] Oskar Klein Centre and Dept. of Physics, Stockholm University, SE-10691 Stockholm, Sweden
[51] Dept. of Astronomy, University of Wisconsin—Madison, Madison, WI 53706, USA
[52] Lawrence Berkeley National Laboratory, Berkeley, CA 94720, USA
[53] Dept. of Physics, Chung-Ang University, Seoul 06974, Republic of Korea
[54] Dept. of Physics, Engineering Physics, and Astronomy, Queen's University, Kingston, ON K7L 3N6, Canada
[55] CTSPS, Clark-Atlanta University, Atlanta, GA 30314, USA
[56] Dept. of Physics, University of Texas at Arlington, 502 Yates Street, Science Hall, Room 108, Box 19059, Arlington, TX 76019, USA
[57] Dept. of Physics, University of Alberta, Edmonton, Alberta, T6G 2E1, Canada
[58] Arthur B. McDonald Canadian Astroparticle Physics Research Institute, Kingston ON K7L 3N6, Canada
[59] Perimeter Institute for Theoretical Physics, Waterloo, ON N2L 2Y5, Canada
[60] Département de physique nucléaire et corpusculaire, Université de Genève, CH-1211 Genève, Switzerland
[61] Columbia Astrophysics and Nevis Laboratories, Columbia University, New York, NY 10027, USA
[62] Dept. of Physics, Yale University, New Haven, CT 06520, USA
[63] Department of Physics, Mercer University, Macon, GA 31207-0001, USA
[64] Dept. of Physics and Astronomy, University of Gent, B-9000 Gent, Belgium
[65] Dept. of Physics and Astronomy, University of Alaska Anchorage, 3211 Providence Drive, Anchorage, AK 99508, USA

[66] Dept. of Physics, University of Oxford, Parks Road, Oxford OX1 3PU, UK
[67] Dept. of Physics, University of Wisconsin, River Falls, WI 54022, USA
Received 2024 June 23; revised 2025 May 21; accepted 2025 May 23; published 2025 July 18

Abstract

The recent IceCube detection of TeV neutrino emission from the nearby active galaxy NGC 1068 suggests that active galactic nuclei (AGNs) could make a sizable contribution to the diffuse flux of astrophysical neutrinos. The absence of TeV γ-rays from NGC 1068 indicates neutrino production in the vicinity of the supermassive black hole, where the high radiation density leads to γ-ray attenuation. Therefore, any potential neutrino emission from similar sources is not expected to correlate with high-energy γ-rays. Disk-corona models predict neutrino emission from Seyfert galaxies to correlate with keV X-rays because they are tracers of coronal activity. Using through-going track events from the Northern Sky recorded by IceCube between 2011 and 2021, we report results from a search for individual and aggregated neutrino signals from 27 additional Seyfert galaxies that are contained in the Swift's Burst Alert Telescope AGN Spectroscopic Survey. Besides the generic single power law, we evaluate the spectra predicted by the disk-corona model assuming stochastic acceleration parameters that match the measured flux from NGC 1068. Assuming all sources to be intrinsically similar to NGC 1068, our findings constrain the collective neutrino emission from X-ray bright Seyfert galaxies in the northern sky, but, at the same time, show excesses of neutrinos that could be associated with the objects NGC 4151 and CGCG 420-015. These excesses result in a 2.7σ significance with respect to background expectations.

Unified Astronomy Thesaurus concepts: Neutrino astronomy (1100); High energy astrophysics (739)

1. Introduction

The IceCube discovery of high-energy cosmic neutrinos (M. G. Aartsen et al. 2013a, 2013b) demonstrated the feasibility of multimessenger astrophysics to find the origin of cosmic rays (CRs; M. Ahlers & F. Halzen 2017). Today, the continuous observation of the high-energy sky by IceCube has revealed evidence for particle acceleration in a nearby Seyfert galaxy, NGC 1068 (R. Abbasi et al. 2022a). This evidence reinforces the idea that active galactic nuclei (AGNs) can generate very-high-energy CRs (F. Halzen & E. Zas 1997) and are potentially the primary contributors to the diffuse neutrino flux observed by IceCube. However, the whereabouts of the remaining sources of the high-energy cosmic neutrino flux remain unknown.

NGC 1068 was identified as the most-significant source in the analysis of nine years of IceCube neutrino observations in the northern sky (R. Abbasi et al. 2022a). The search identified an excess of 79 events in the direction of NGC 1068 corresponding to a muon neutrino flux of $5 \times 10^{-14}\,\mathrm{GeV^{-1}\,cm^{-2}\,s^{-1}}$ at 1 TeV with the best-fit power-law spectral index of 3.2. The neutrino flux measured from NGC 1068 is much larger than the γ-ray emission in TeV energies if extrapolated from the $\sim$GeV γ-ray emission measured by Fermi Large Area Telescope (S. Abdollahi et al. 2020; J. Ballet et al. 2020). It is also more than an order of magnitude larger than the upper limits placed by MAGIC and HAWC (V. A. Acciari et al. 2019; E. Willox et al. 2022) on $\sim$TeV γ-ray emissions. High-energy neutrinos and γ-rays are simultaneously produced whenever CRs interact with ambient matter or radiation within or near cosmic accelerators (F. Halzen & A. Kheirandish 2019). The observed difference between neutrinos and γ-rays from NGC 1068 cannot be explained by absorption by the extragalactic background light (EBL; K. Murase 2022a). Therefore, the environments where the neutrinos are produced in NGC 1068 must be opaque to GeV–TeV γ-rays that would otherwise accompany the neutrinos. Among the primary candidates are the cores of AGNs, which can simultaneously accommodate the efficient production of high-energy neutrinos and offer an optically thick zone that obscures the accompanying γ-rays. Consequently, the observed $\sim$GeV γ-rays should have a different origin than the observed neutrinos (K. Murase et al. 2020).

The high level of neutrino emission compared to γ-rays from NGC 1068 is in agreement with the multimessenger picture for the total diffuse high-energy neutrino flux reported by IceCube (M. G. Aartsen et al. 2020b; R. Abbasi et al. 2022b). This isotropic neutrino flux is an order of magnitude greater at medium energies ($\sim$30 TeV) than it is at very high energies (>100 TeV) (M. G. Aartsen et al. 2020a). Comparisons between the diffuse neutrino flux at medium energies and the isotropic γ-ray background observed by Fermi (M. Ackermann et al. 2015) independently suggest neutrino production in environments that are obscured to high-energy γ rays (N. Senno et al. 2015; K. Murase et al. 2016; K. Bechtol et al. 2017; A. Capanema et al. 2020; K. Fang et al. 2022), in line with the previously discussed multimessenger picture of NGC 1068.

AGNs host supermassive black holes at their centers that power these galaxies via the release of gravitational energy from accreting matter. The accreting matter falls toward the black hole and forms a disk around the central engine, i.e., the core of the AGN. The cores of AGNs are optically thick for GeV–TeV γ-rays. Simultaneously, they provide the target matter and radiation that is required for the efficient production of neutrinos. See K. Murase & F. W. Stecker (2023) and references therein for more details.

IceCube has previously searched for the collective neutrino flux from AGN cores by considering a large catalog of AGNs and assuming that neutrinos are produced by accelerated CRs

[68] also at Institute of Physics, Sachivalaya Marg, Sainik School Post, Bhubaneswar 751005, India.
[69] also at Department of Space, Earth and Environment, Chalmers University of Technology, 412 96 Gothenburg, Sweden.
[70] also at Earthquake Research Institute, University of Tokyo, Bunkyo, Tokyo 113-0032, Japan.

in the AGN accretion disks (R. Abbasi et al. 2022c). In the study presented here, motivated by the observation of ∼TeV neutrinos from NGC 1068, which is among the brightest AGNs in intrinsic X-rays (F. E. Bauer et al. 2015; A. Marinucci et al. 2016; C. Ricci et al. 2017), we instead aim to identify neutrino emission from a targeted selection of X-ray bright Seyfert galaxies in the northern sky (decl. $> -5°$). In particular, our selection focuses on the 2–10 keV energy range which, in a $p\gamma$ scenario, would provide the target photons with the right energy to efficiently produce ∼TeV neutrinos (D. F. G. Fiorillo et al. 2024; P. Padovani et al. 2024) and thus generally make X-rays a principal proxy of neutrino emission. In addition, the same X-rays would simultaneously absorb the high-energy γ-rays (K. Murase et al. 2020). In our study, each candidate source is then searched individually for signs of point-like neutrino emission above background expectations. Here, in addition to the generic power-law spectral assumption, we turn our attention to neutrino emission from the coronae of Seyfert galaxies (K. Murase et al. 2020; A. Kheirandish et al. 2021). In this search, we employ model-predicted neutrino spectra accounting for CR interactions with ambient matter and radiation in the coronal environment, as well as the generic single power-law flux. Additionally, we perform a joint analysis of all sources using a *stacking* method to search for potential collective emissions from these sources.

In the next section, we discuss neutrino emission from the coronae of bright Seyfert galaxies. In Section 3 we present details about the source selection and analysis methods. The results of each test performed in this study are presented in Section 4. In Section 5 we discuss the implication of each analysis.

2. Seyfert Galaxies as Sources of High-energy Neutrinos

In Seyfert galaxies, accretion dynamics and magnetic dissipation lead to the formation of a hot, highly magnetized, and turbulent corona above the disk; see, e.g., K. Miller & J. Stone (2000). The dense environments near the supermassive black holes together with the acceleration of CRs in the coronae offer suitable conditions for the production of high-energy neutrinos. Simultaneously, these systems will be opaque to the accompanying very-high-energy γ-rays. Such a scenario has been examined by models that attempt to describe the neutrino flux at the medium energy range of the IceCube high-energy diffuse astrophysical neutrino observation and the soft best-fitted spectrum reported from NGC 1068 (Y. Inoue et al. 2020; K. Murase et al. 2020; A. Kheirandish et al. 2021; B. Eichmann et al. 2022). These models, commonly referred to as disk-corona models, can accommodate the high level of neutrino emission at medium energies and the measured neutrino flux from NGC 1068; see, e.g., K. Murase & F. W. Stecker (2023) for detailed discussion. Disk-corona models are, however, not the only possibility; see, e.g., S. Inoue et al. (2023) for a different scenario with similar phenomenology. Here, we focus on the disk-corona model presented by K. Murase et al. (2020) and A. Kheirandish et al. (2021) where neutrino emission is a product of stochastic acceleration in the corona and interaction of CRs with gas or the radiation from the innermost regions of the AGN. On the basis of the reported intrinsic X-ray flux, this model finds NGC 1068 as the brightest source in IceCube and suggests that additional sources might be identified in IceCube if they pose similar characteristics to NGC 1068.

AGN coronae are primarily characterized by X-ray emission that is powered thermally. In the scenario discussed in this work, the CR injection fraction is proportional to the dissipation rate in the coronae, which is determined by the thermal X-ray luminosity. Naturally, the intrinsic X-ray luminosity becomes the principal parameter in the disk-corona models for estimating the neutrino emission. Additional model parameters include the CR to thermal pressure ratio that summarizes the CR budget and the turbulence strength. Larger values of this ratio result in increased neutrino production. While moderate values can explain the diffuse neutrino flux at medium energies, a higher level of CR pressure is needed to explain the neutrino flux measured in the direction of NGC 1068 (A. Kheirandish et al. 2021). This assumption is heavily tied to the measured X-ray flux, and we will return to it in the discussion of the results. For this study, we solely focus on the high CR pressure scenario (i.e., $P_{\rm CR}/P_{\rm th} = 50\%$) with corresponding turbulent strength ($\eta_{\rm tur}$) of 50 since the identification of sources with moderate CR pressure requires next-generation neutrino telescopes (A. Kheirandish et al. 2021).

3. Searching for Neutrino Emission from Bright Seyfert Galaxies in the Northern Sky

3.1. Source Catalog

Our source catalog is based on the Swift's Burst Alert Telescope (BAT) AGN Spectroscopic Survey (BASS; C. Ricci et al. 2017) which is an all-sky study of AGNs detected in the X-ray band. In our selection, we start from all sources identified as Seyfert galaxies with the 105 month Swift-BAT classification (K. Oh et al. 2018). BAT sources in the northern sky (decl. $> -5°$) are ranked by their intrinsic X-ray fluxes in the 2–10 keV band. Sources with weak intrinsic X-ray fluxes are not expected to produce sizeable neutrino fluxes. Therefore, we select only bright sources for our analysis with intrinsic X-ray fluxes that are at least 10% that of NGC 1068, which is approximately the sensitivity of IceCube in the northern sky according to the previous result of NGC 1068 (R. Abbasi et al. 2022a). The selection retains 28 sources including NGC 1068. Considering the a priori knowledge of a strong flux from this source, we separate out the results for NGC 1068 to avoid bias in the analysis. Therefore, we discuss the exclusion and inclusion of NGC 1068 separately. To be conservative and to take into account the fact that the remaining sources can still give neutrino signals significant enough based on the model, we draw our conclusion without NGC 1068, and the results including NGC 1068 are shown for completeness.

3.2. IceCube Detector and Data

The IceCube Neutrino Observatory at the South Pole is a Cherenkov neutrino telescope that utilizes 1 km^3 volume of glacial ice to detect high-energy neutrinos. The detector is an array of 5160 digital optical modules (DOMs), each composed of a photomultiplier tube (PMT) and onboard read-out electronics (M. G. Aartsen et al. 2017). Cherenkov photons emitted by the relativistic charged particles produced in interactions between neutrinos and nucleons are collected by the PMTs. The photon count and arrival time recorded by each DOM are used to reconstruct the energy and direction of each event. The flavors and interaction types of neutrinos lead to different event morphologies in the detector. Among them, track events resulting from charged-current interactions of muon neutrinos can be reconstructed with good angular resolutions (R. Abbasi et al. 2022a), which makes them ideal for pointing back to their sources. However, muons and neutrinos produced in the atmosphere present a significant background. Fortunately, the Earth acts as an effective muon filter for up-going events from the northern sky, thus a better sensitivity can be reached due to the suppression of the atmospheric muon background. Here, we analyze the through-going muon tracks in the northern sky (decl. $> -5^{\circ}$, R. Abbasi et al. 2022b).

The data sample is processed in the same way as in R. Abbasi et al. (2022a) which has new data processing, data calibration, and event reconstruction implemented that result in substantially improved energy reconstructions and point-spread function at low to medium energies. The details can be found in the supplementary materials of R. Abbasi et al. (2022a). We extend the data used in this previous work by adding extra 1.7 yr of experimental data. We also improved the modeling of the muon contribution from the decay of tau leptons produced by tau neutrino charged-current interactions outside the detector by adding dedicated Monte Carlo (MC) simulations. The extension of the lifetime increases the total number of events by ∼20%. The experimental data starts with the fully built and commissioned detector (aka IC86) on 2011 May 13 and ends on 2022 February 13 with a total live time of 3804 days, corresponding to 794,301 track events in total.

3.3. Analysis

In order to discriminate between potential neutrino emission from our selected sources and the background composed of atmospheric and isotropic astrophysical neutrinos, we employ the unbinned likelihood ratio hypothesis testing method that utilizes the direction, energy proxy, and angular uncertainty of the events (J. Braun et al. 2008). We perform two types of searches. One is the catalog search, where we look for the neutrino emission from each source separately, using both a power-law assumption and disk-corona model prediction. The outcome will be used to conduct a binomial test to examine the significance of observing excesses for k sources in these two scenarios for our catalog search. This could potentially identify a subset of sources that do not individually pass the significance threshold. The other is the stacking search, where the emission of each selected source is combined according to model expectations in order to obtain an enhanced signal above the background. In the stacking analysis, only the disk-corona model flux is tested. All searches were specified a priori.

These analyses apply the improved kernel density estimation (KDE) method presented in R. Abbasi et al. (2022a) to generate probability density functions (PDFs), which improves the modeling of directional distributions of individual neutrinos. These distributions depend on the shape of the spectrum and were therefore generated for each spectral index in the power-law flux analysis (R. Abbasi et al. 2022a). Using the same methods, we generate the signal spatial PDFs corresponding to the disk-corona model spectra with an updated KDE generation pipeline, where we utilize a grid in the intrinsic X-ray luminosity L_X, the parameter that determines the shape of the flux. In the catalog search, under the assumption of a single power-law flux, we determine two fit parameters for each source: the number of expected signal events n_s and the spectral index γ. In addition, we fit the observations from each source with the flux predicted by the disk-corona model. Here, the shape of the flux is fixed by the intrinsic X-ray luminosity L_X taken from BASS. Hence, there is only one fit parameter corresponding to the normalization (and therefore the cosmic-ray pressure): the number of expected signal events n_s. The same is done in the stacking analysis, which is based on the same model. We fit the global number of signal events n_s (total contribution from all sources), while the relative sources weights and flux shapes are fixed by the model predictions and the observed X-ray luminosities. More details about the likelihood method can be found in the Appendix.

For the analyses based on the disk-corona model, we calculate the expected number of events from each source with the high-pressure scenario described in A. Kheirandish et al. (2021), and thus assume that all sources behave intrinsically similar to NGC 1068. Here, the flux shape is fixed by L_X, and the flux normalization changes with the CR pressure. The expected fluxes of selected sources are shown in Figure 1. The total model fluxes with and without NGC 1068 for the stacking search are also shown with comparison to the 5σ discovery potential, where a 6σ significance is expected even without NGC 1068 for the optimistic scenario. Testing the performance of the analysis shows that if the disk-corona model predicts the true flux, modeling the flux correctly gives a gain of $\sim 1\sigma$ significance for the stacking search and $\sim 0.7\sigma$ for NGC 1068 compared to fitting a power-law spectrum, as can be seen in Figure 7 in the Appendix.

For the catalog search based on the power-law spectrum assumption, we follow the same procedure as in R. Abbasi et al. (2022a). This analysis complements the search discussed above for possible high-energy events if neutrino emission from any of the sources is extended to above ∼100 TeV, and thus offer an intuitive comparison with other work by applying the generic power-law flux assumption.

4. Results

Table 1 shows a summary of our results. In addition to NGC 1068, we find excesses of neutrino emission that could be associated with two other sources: CGCG 420-015 and NGC 4151. CGCG 420-015 is the most-significant source in the search based on the disk-corona model with a 3.5σ local (pretrial) significance, while NGC 4151 stands out as the most-significant source in the search based on the power-law spectrum assumption with a 3.2σ local significance. Starting from the larger value 3.5σ, the global significance is lowered by the *look-elsewhere effect* by accounting for the number of objects in the catalog (27) and the two spectral assumptions. The global significance of the catalog search is 2.3σ, as determined by repeated applications of the entire analysis to simulated data containing only background events.

The local significance of NGC 1068 increases slightly compared to the previous result in R. Abbasi et al. (2022a) due to the extension of the data set. Assuming the power-law spectral model, we obtain a local p-value of 8×10^{-8}, which corresponds to a global significance of 4.3σ in the previous catalog search described in R. Abbasi et al. (2022a) ($N = 110$ candidate sources) and is consistent with expectations assuming the best-fitting values in the previous analysis. The panels in Figure 2 display the p-value scan in the nearby region

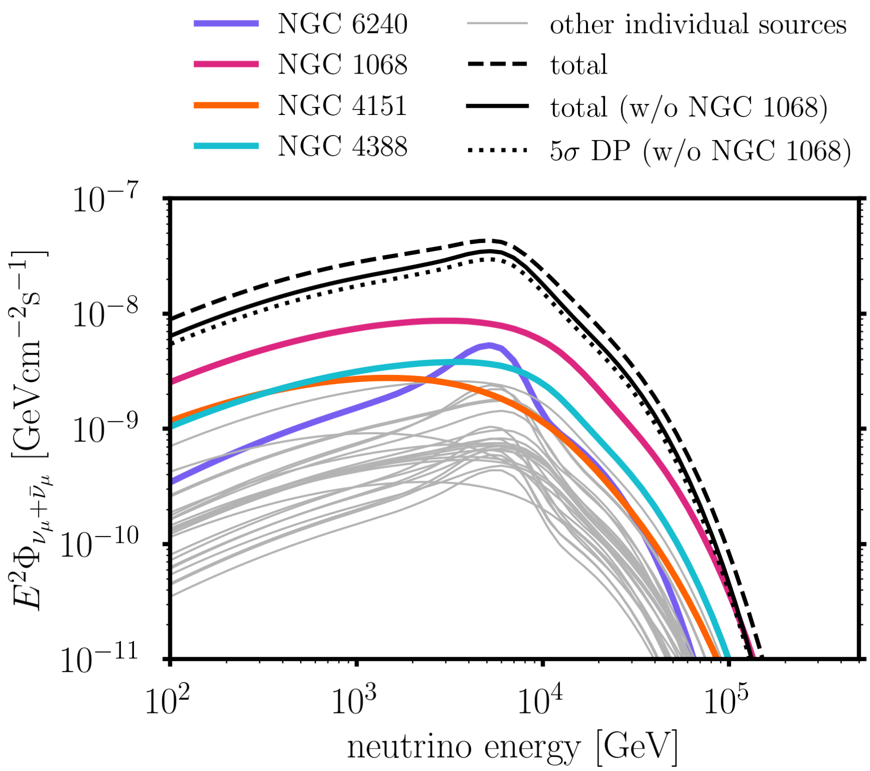

Figure 1. The expected flux of each source (thin lines) from the disk-corona model (high CR pressure) with the top four sources highlighted. The total fluxes excluding or including NGC 1068 are shown. The 5σ discovery potential (DP), which excludes NGC 1068, is given as well.

Table 1
Results

	Spectral Model	$n_{\rm exp}$	TS	$\hat{n}_s$	$\hat{\gamma}$	$p_{\rm local}$	$p_{\rm global}$	$n_{\rm UL}$
Stacking Searches								
Stacking (excl.)	Disk-corona	154.0	0.1	5	⋯	2.4×10^{-1} (0.7σ)	2.4×10^{-1} (0.7σ)	51.1
Stacking (incl.) $^{(*)}$	Disk-corona	199.0	11.2	77	⋯	1.1×10^{-4} (3.7σ)	⋯	128.0
Catalog Search 1								
CGCG 420-015	Disk-corona	3.2	11.0	31	⋯	2.4×10^{-4} (3.5σ)	6.5×10^{-3} (2.5σ)	46.4
NGC 4151	Disk-corona	13.1	9.0	23	⋯	6.4×10^{-4} (3.2σ)	⋯	39.5
NGC 1068 $^{(*)}$	Disk-corona	44.6	23.4	48	⋯	3.0×10^{-7} (5.0σ)	⋯	61.4
Catalog Search 2								
NGC 4151	Power-law	⋯	7.4	30	2.7	6.4×10^{-4} (3.2σ)	1.7×10^{-2} (2.1σ)	61.4
CGCG 420-015	Power-law	⋯	9.2	35	2.8	3.0×10^{-3} (2.7σ)	⋯	62.1
NGC 1068 $^{(*)}$	Power-law	⋯	29.5	94	3.3	8.0×10^{-8} (5.2σ)	⋯	94.9
Binomial Searches								
Binomial Search 1 (excl.)	Disk-corona	⋯	⋯	⋯	⋯	1.4×10^{-4} ($k = 2$)	1.7×10^{-3} (2.9σ)	⋯
Binomial Search 2 (excl.)	Power-law	⋯	⋯	⋯	⋯	1.2×10^{-3} ($k = 3$)	1.4×10^{-2} (2.2σ)	⋯

Note. Results for the stacking search and selected results from two catalog searches, Catalog Search 1: disk-corona model and Catalog Search 2: power-law model, and corresponding binomial tests, Binomial Search 1: disk-corona model and Binomial Search 2: power-law model. Best-fitted TS, $\hat{n}_s$, local (pretrial) and global (post-trial) p-values, and corresponding significances are shown. For the disk-corona model analysis, expected numbers of events ($n_{\rm exp}$) are listed and for the power-law analysis, best-fitted spectral indices $\hat{\gamma}$ are listed. $n_{\rm UL}$ column shows the 90% upper limits of the numbers of signal events. Upper limits assuming power-law spectra are given assuming E^{-3}. Results marked with $^{(*)}$ are provided for completeness but are not used to compute final significances because evidence for neutrino emission from NGC 1068 was known prior to this work (M. G. Aartsen et al. 2020c; R. Abbasi et al. 2022a). For the binomial tests, the value k corresponds to the number of sources retained in the most-significant set (see Appendix for details).

around the most-significant sources under our two spectral assumptions. Their best-fit fluxes are shown in Figure 3 where the model fit and power-law fit can be compared. The profile likelihood scans for the powerlaw fit are shown in Figure 8 in the Appendix. The fluxes given by the model fit can also be compared to their expected spectra. For all selected sources,

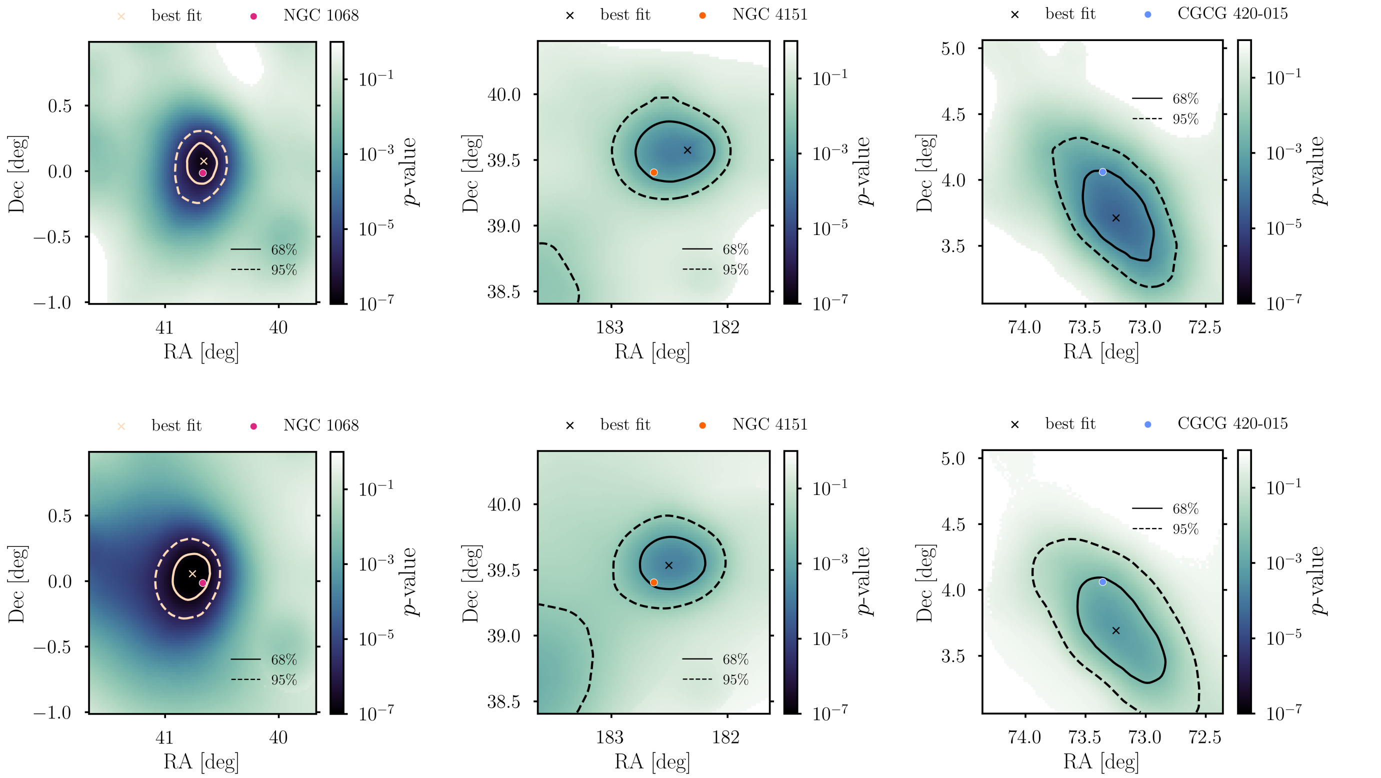

Figure 2. Local (pretrial) p-value maps around the most significance sources NGC 1068 (left), NGC 4151 (middle), and CGCG 420-015 (right) with the disk-corona model fit (top) and the power-law fit (bottom). Colored points show the locations of sources and crosses show the best-fit locations. Contours correspond to 68% (solid) and 95% (dashed) confidence regions.

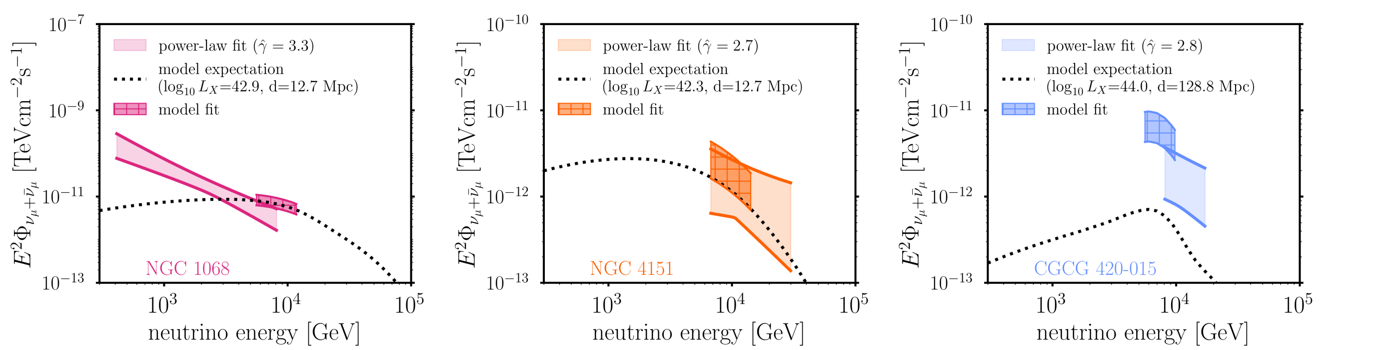

Figure 3. The best-fitted flux and the corresponding 68% statistical uncertainty for model and power-law searches compared to the expected disk-corona flux for the most-significant sources NGC 1068 (left), NGC 4151 (middle), and CGCG 420-015 (right). Distance and intrinsic X-ray luminosity (in erg s^{-1}) for each source are taken from BASS. Systematic uncertainties are subdominant. The neutrino energy range of the best-fitted flux is computed from the 68% central bins contribution to the total TS value. See the Appendix for more details about the determination of the energy range and the description of systematic uncertainties.

Figure 4 compares the expected number of events to the measurements consisting of either the computed 90% confidence level upper limits or the best-fit flux value (NGC 1068). The model prediction, based on stochastic particle acceleration and high cosmic-ray pressure in the AGN corona, appears to be ruled out for NGC 6240 and NGC 4388 because the 90% CL upper limits are below the expected fluxes for these two candidate sources. The full information and results for all sources are tabulated in Table 2.

The binomial test (M. G. Aartsen et al. 2019) allows us to combine these results without any assumption about the relative contribution from the candidate sources in our catalog. Assuming the disk-corona flux model for each candidate source, and excluding NGC 1068, we find a combined pretrial significance of 2.9σ in excess of the expected backgrounds. For the generic power-law flux, the same test yields a pretrial significance of 2.2σ. After accounting for having tested the two flux models (and the associated trials factor), the global significance of the binomial test becomes 2.7σ. This result rests on the observation of two candidate sources ($k = 2$) with small local p-values in our catalog: NGC 4151 and CGCG 420-015. Including NGC 1068 would increase the number of sources, identified in this test, by one ($k = 3$), and result in an a posteriori significance of 4σ. For more details about the binomial test and this result, see the Appendix.

As can be seen in Table 1, there is no significant excess found in the stacking search without contribution from NGC 1068 with p-value = 0.24. The 90% C.L. upper limit

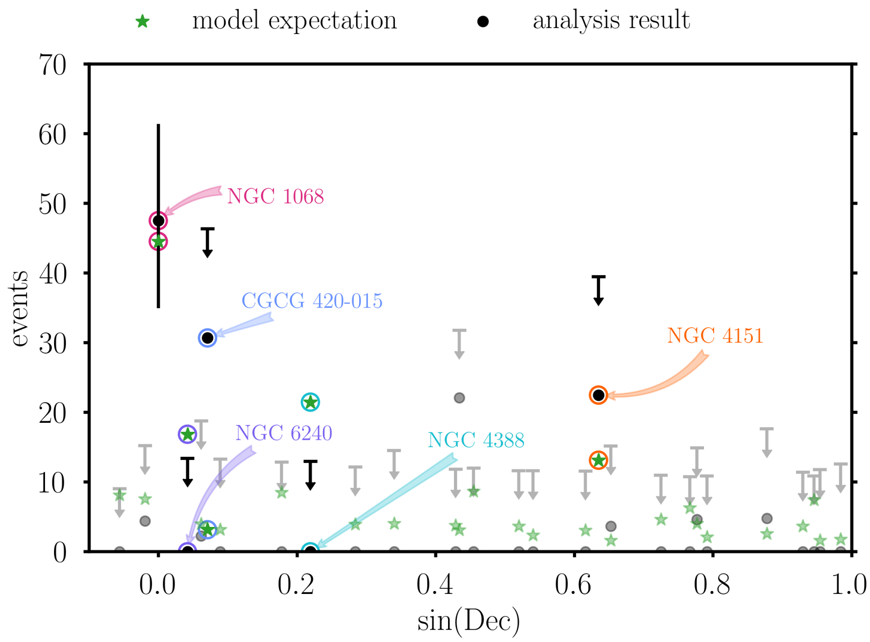

Figure 4. Expected numbers of events (green stars) from the model and the best-fitted numbers of signal events (black circles) for individual sources. Down arrows show the 90% C.L. upper limits. The five candidate sources with the strongest expected neutrino signal (disk-corona model) are highlighted.

Table 2
Source List and Results

Source	Decl.	R.A.	$F^{\rm intr}_{2-10\,{\rm keV}}$	$n_{\rm exp}$	Model $\hat{n}_s$	-log$_{10}p$	$n_{\rm UL}$	$\hat{n}_s$	$\hat{\gamma}$	Power Law -log$_{10}p$	$\phi^{E^{-2}}_{90\%}$	$\phi^{E^{-3}}_{90\%}$
NGC 1068	−0.0	40.7	268.3	44.5	47.5	6.5	61.4	94.1	3.3	7.1	8.5	449.0
NGC 4388	12.7	186.4	71.7	21.4	0.0	0.0	13.0	2.0	1.9	0.9	3.9	130.0
NGC 6240	2.4	253.2	411.1	16.8	0.0	0.0	13.4	0.0	4.3	0.0	1.5	60.9
NGC 4151	39.4	182.6	84.8	13.1	22.5	3.2	39.5	30.1	2.7	3.2	10.9	214.0
Z164-19	27.0	221.4	179.5	8.6	0.0	0.0	12.0	3.3	2.0	0.7	4.2	99.1
UGC 11910	10.2	331.8	157.5	8.5	0.0	0.0	12.9	6.4	4.3	0.3	2.2	69.2
NGC 5506	−3.2	213.3	115.6	8.1	0.0	0.0	9.0	0.0	1.6	0.0	1.9	102.5
NGC 1194	−1.1	46.0	117.8	7.6	4.4	0.6	15.2	27.7	3.7	0.9	2.9	161.5
Mrk3	71.0	93.9	113.6	7.4	0.0	0.0	10.9	0.0	4.3	0.0	4.4	46.4
MCG+8-3-18	50.1	20.6	99.4	6.3	0.0	0.0	10.8	0.0	4.3	0.0	3.3	47.6
UGC 3374	46.4	88.7	65.1	4.6	0.0	0.0	11.0	0.0	4.3	0.0	3.2	46.9
NGC 3227	19.9	155.9	37.2	4.0	0.0	0.0	14.5	0.0	1.7	0.0	2.1	46.7
4C+50.55	51.0	321.2	97.0	4.0	4.6	0.8	14.9	9.7	3.2	0.5	5.0	78.9
NGC 7682	3.5	352.3	47.9	4.0	2.3	0.7	18.8	0.0	4.3	0.0	1.6	62.4
IRAS05078+1626	16.5	77.7	46.1	4.0	0.0	0.0	12.2	0.0	4.3	0.0	2.0	50.0
2MASX J20145928+2523010	25.4	303.7	78.6	3.8	0.0	0.0	11.9	0.0	4.3	0.0	2.3	47.9
Mrk 1040	31.3	37.1	40.6	3.7	0.0	0.0	11.7	32.9	4.3	0.9	5.1	114.0
LEDA136991	68.4	6.4	42.6	3.7	0.0	0.0	11.4	3.8	4.1	0.2	5.0	53.9
Mrk 1210	5.1	121.0	32.9	3.2	0.0	0.0	13.3	0.0	4.3	0.0	1.7	60.1
CGCG 420-015	4.1	73.4	50.5	3.2	30.7	3.6	46.4	35.5	2.8	2.5	5.2	254.6
MCG+4-48-2	25.7	307.1	31.6	3.1	22.1	2.3	31.8	45.2	3.2	2.1	7.2	182.5
3C111	38.0	64.6	61.5	3.1	0.0	0.0	11.6	15.7	4.3	0.5	4.2	76.2
UGC 5101	61.4	144.0	45.4	2.6	4.8	1.0	17.6	8.7	3.0	0.7	6.9	95.2
3C382	32.7	278.8	49.4	2.4	0.0	0.0	11.6	34.9	4.3	1.0	5.4	118.2
Mrk 110	52.3	141.3	34.4	2.1	0.0	0.0	10.9	0.0	4.3	0.0	3.4	47.9
3C 390.3	79.8	280.5	44.4	1.8	0.0	0.0	12.6	0.0	4.3	0.0	6.9	78.6
NGC 3516	72.6	166.7	30.7	1.6	0.0	0.0	11.8	30.0	4.3	0.6	8.8	104.7
Cygnus A	40.7	299.9	32.1	1.6	3.7	0.7	15.2	2.9	2.1	0.7	5.3	97.2

Note. Information of sources and the catalog search results. Intrinsic 2–10 keV X-ray flux is $F^{\rm intr}_{2-10\,{\rm keV}} \times 10^{-12}$ erg cm^{-2}s^{-1}. Best-fit results for TS, $\hat{n}_s$ and pretrial p-values for both the model analysis and power-law spectral assumptions are shown. For the model analysis, expected numbers of signal events ($n_{\rm exp}$) and 90% upper limit of the signal event numbers ($n_{\rm UL}$) are listed and for the power-law analysis, best-fitted spectral indices $\hat{\gamma}$ and 90% upper limit fluxes are listed. The upper limit fluxes are parameterized as $\phi^{E^{-\gamma}}_{90\%}(E/1\ {\rm TeV})^{-\gamma} \times 10^{-13}$ TeV^{-1}cm^{-2}s^{-1}.

on the total number of signal neutrinos from the selection of sources excluding NGC 1068 is $n_s^{\rm UL} = 51$, while $n_{\rm exp} = 155$ events were expected had all analysis assumptions been met exactly. If NGC 1068 is included, the upper limit becomes $n_s^{\rm UL} = 128$ compared to an expectation of $n_{\rm exp} = 199$.

5. Discussion

In this study, we probed neutrino emission in the direction of the brightest Seyfert galaxies identified in the BASS catalog. Based on the disk-corona model prediction, collective emission from these sources should emerge with high significance in IceCube data provided that the sources are characterized by a high CR pressure, similar to NGC 1068. On the one hand, taking the intrinsic X-ray luminosities and distances reported by BASS (C. Ricci et al. 2017) at face value, the absence of a strong signal in the stacking search implies that the model parameters that are suited to explain the observed flux from NGC 1068 appear not to be shared with most sources in the catalog. On the other hand, the results of the catalog searches, in particular the 2.7σ neutrino excess in the binomial test, may suggest the existence of a subset of Seyfert galaxies that are similar to NGC 1068, which would add to the growing indications that at least a subset of AGNs contribute to the high-energy neutrino flux. However, more data is needed for a robust identification of these and other similar sources.

The first implication of the aforementioned results is that the CR to thermal pressure parameter, which sets the normalization of CRs at the source, may be lower than what is projected for NGC 1068. Sources with lower values are beyond the reach of the current generation of neutrino telescopes, and their identification would be feasible with the commissioning of IceCube-Gen2 (A. Kheirandish et al. 2021).

Both the selection of the X-ray bright Seyfert galaxies in this study and the expected neutrino flux in the disk-corona model, depend strongly on the reported intrinsic X-ray flux in BASS. Therefore, the accuracy of the reported estimates for the intrinsic X-ray emission becomes one of the main hurdles and the primary source of astrophysical systematic uncertainty in this analysis. Among the most promising candidate sources that are considered in this analysis are Compton thick AGNs, i.e., AGNs with high levels of X-ray obscuration (column density $N_{\rm H} \gtrsim 10^{24}\,{\rm cm}^{-2}$), for which the assessment of the intrinsic luminosity is challenging. This includes CGCG 420-015, for which the estimated neutrino flux, if interpreted as a genuine signal, would exceed the model expectation by about an order of magnitude. The BASS catalog that is utilized in this analysis offers the most comprehensive survey of nonjetted AGN. However, the accurate measurement of the intrinsic X-ray flux from Compton thick sources requires careful modeling that can benefit from additional data, especially targeting instruments such as NuStar that are sensitive to higher energy X-rays. It is worth mentioning that detailed modeling of a few of the prominent sources in these searches (A. Tanimoto et al. 2022) yields an intrinsic flux that is not compatible with BASS. For example, the higher intrinsic flux reported for NGC 1068 (A. Marinucci et al. 2016) would, compared to BASS, prefer a lower value of CR pressure within the disk-corona model to describe the neutrino flux. Correspondingly, adopting a lower value for the rest of the sources would decrease the expected emission from these other sources in the catalog. Similarly, the discrepancy between different measurements of the intrinsic luminosity for the rest of the sources would change their expected neutrino fluxes. For a recent evaluation of the intrinsic X-ray luminosity of Compton thick AGNs, see A. Tanimoto et al. (2022). Additional studies are particularly encouraged in light of the absence of a detectable neutrino signal in the direction of NGC 4388. Given its proximity, and the high level of intrinsic X-ray flux reported by BASS, the disk-corona model with high CR pressure predicts 21 events from NGC 4388, making it the brightest source in our list excluding NGC 1068. A recent dedicated analysis of the intrinsic emission from this source, however, reports a lower value for the intrinsic flux and a drop during the period of this analysis (N. Torres-Albà et al. 2023). A reduction in X-ray emissivity during the IceCube data taking period would lower the predicted neutrino emission and would be consistent with the nonobservation of neutrinos reported here for this source (N. Torres-Albà et al. 2023). In summary, a more accurate measurement of the intrinsic X-ray flux from these sources will likely modify the expected emission from the Seyfert galaxies and the prospects for identifying them. The stacking analysis in particular is highly dependent on these uncertainties, in addition to the assumption that the sources have a high CR pressure.

Finally, we should also note that the uncertainties in model parameters, such as the size of the corona and underlying diffusion, could change the expected neutrino flux and subsequently the likelihood for observation of the sources. The search in this study assumes that sources share the same underlying model parameters, which is a strong assumption. For more detailed study of the underlying parameters; see, e.g., K. Murase (2022b, 2024), M. Ajello et al. (2012), and A. Das et al. (2024).

6. Summary and Outlook

In this work, we present a study of potential high-energy neutrino emission from Seyfert galaxies in the northern sky that are intrinsically X-ray bright. In addition to the generic power-law flux assumption, we incorporate the disk-corona model and performed a catalog search with 27 (28) sources excluding (including) NGC 1068. We also performed a search for aggregated neutrino emission using a stacking method relying on the disk-corona flux model. Since there is no significant excess of neutrino events observed in the stacking search, we can constrain the collective neutrino emission from those X-ray bright Seyfert galaxies in the northern sky.

Since we cannot reject the null hypothesis, we set upper limits on the neutrino emission from all individual sources for both scenarios. The current results motivate continuing searches for neutrino emission from X-ray bright Seyfert galaxies in addition to NGC 1068, especially NGC 4151 and CGCG 420-015, which will reveal whether the cumulative 2.7σ excess reported here is due to statistical fluctuations or a genuine astrophysical signal. If interpreted as the latter, it would suggest the existence of sources similar to NGC 1068, which could potentially be explained by the disk-corona model. Nevertheless, the absence of a significant correlation in the stacking search and most individual sources implies that the features of NGC 1068 leading to the strong neutrino emission are not commonly shared with other X-ray bright Seyfert galaxies. As discussed in Section 5, the expectation of neutrino emission relies considerably on the details of the modeling within the picture of the disk-corona model, and more comprehensive multiwavelength observations will provide further insight into the characteristics of the potential sources, which is expected to significantly improve their modeling. The results reported here show that implementing dedicated models is useful and can improve the sensitivity of searches for the sources of high-energy neutrinos.

Our conclusions are supported by a complementary IceCube study of hard X-ray (14-195 keV) AGNs, identified in BASS, which reports an excess of neutrinos toward NGC 4151 at 2.9σ post-trial significance (R. Abbasi et al. 2025). This analysis is based on an alternative track event selection (M. G. Aartsen et al. 2020b) that includes data from the entire sky recorded during partial detector configurations before IceCube was fully commissioned. While this study employs a different hypothesis, data sample, and analysis techniques, the results of the catalog search are consistent with the results reported here.

IceCube-Gen2, the next-generation of the IceCube detector (M. G. Aartsen et al. 2021), will be 8 times larger in volume with an expected 5 times increase of the effective area for muon tracks, increasing the potential to discover neutrino sources by a factor of $\sim$5. This improvement could lead to the discovery of neutrino emission from the interesting sources studied in this work.

Considering the fact that the majority of bright Seyfert galaxies, the Circinus galaxy for example, reside in the southern sky, an enhanced sensitivity toward that region would help the search for more sources similar to NGC 1068. The recent technical progress in starting track and cascade event selections in IceCube (R. Abbasi et al. 2021, 2023, 2024) provides significantly improved sensitivity to the southern sky, thus creating an excellent opportunity to search for neutrino emission from these interesting southern sky sources. In the upcoming years, detectors built, or under construction, in the northern sky such as Baikal-GVD, KM3NeT, P-ONE, and TRIDENT (S. Adrian-Martinez et al. 2016; A. D. Avrorin et al. 2018; M. Agostini et al. 2020; Z. P. Ye et al. 2023) will further boost the identification of sources in the southern sky.

Acknowledgments

The authors gratefully acknowledge the support from the following agencies and institutions: USA—U.S. National Science Foundation-Office of Polar Programs, U.S. National Science Foundation-Physics Division, U.S. National Science Foundation-EPSCoR, U.S. National Science Foundation-Office of Advanced Cyberinfrastructure, Wisconsin Alumni Research Foundation, Center for High Throughput Computing (CHTC) at the University of Wisconsin–Madison, Open Science Grid (OSG), Partnership to Advance Throughput Computing (PATh), Advanced Cyberinfrastructure Coordination Ecosystem: Services & Support (ACCESS), Frontera Computing Project at the Texas Advanced Computing Center, U.S. Department of Energy-National Energy Research Scientific Computing Center, Particle Astrophysics Research Computing Center at the University of Maryland, Institute for Cyber-Enabled Research at Michigan State University, Astroparticle Physics Computational Facility at Marquette University, NVIDIA Corporation, and Google Cloud Platform; Belgium—Funds for Scientific Research (FRS-FNRS and FWO), FWO Odysseus and Big Science programmes, and Belgian Federal Science Policy Office (Belspo); Germany—Bundesministerium für Bildung und Forschung (BMBF), Deutsche Forschungsgemeinschaft (DFG), Helmholtz Alliance for Astroparticle Physics (HAP), Initiative and Networking Fund of the Helmholtz Association, Deutsches Elektronen Synchrotron (DESY), and High Performance Computing cluster of the RWTH Aachen; Sweden—Swedish Research Council, Swedish Polar Research Secretariat, Swedish National Infrastructure for Computing (SNIC), and Knut and Alice Wallenberg Foundation; European Union—EGI Advanced Computing for Research; Australia—Australian Research Council; Canada—Natural Sciences and Engineering Research Council of Canada, Calcul Québec, Compute Ontario, Canada Foundation for Innovation, WestGrid, and Digital Research Alliance of Canada; Denmark—Villum Fonden, Carlsberg Foundation, and European Commission; New Zealand—Marsden Fund; Japan—Japan Society for Promotion of Science (JSPS) and Institute for Global Prominent Research (IGPR) of Chiba University; Korea—National Research Foundation of Korea (NRF); Switzerland—Swiss National Science Foundation (SNSF).

Appendix

The analysis presented here is an extension of the one described in R. Abbasi et al. (2022a). First, we increased the number of neutrino events from $\sim$665,000 to $\sim$794,000 by adding data recorded by IceCube during an additional period of 1.7 yr. Second, in addition to the generic power-law spectral assumption, we studied a specific model (K. Murase et al. 2020; A. Kheirandish et al. 2021) that relates intrinsic X-ray fluxes to expected neutrino fluxes from the coronal regions of bright Seyfert galaxies. All other technical aspects, such as the event selection criteria and the likelihood function, remain identical. Increasing the available live time by $\sim$20% improves the 5σ discovery potential of the analysis by $\sim$10%, as shown in Figure 5 for a single power-law spectral assumption with spectral indices $\gamma = 2.0$ (left) and $\gamma = 3.2$ (right).

The KDEs of the signal and background PDFs that govern the reconstructed muon directions and energies, developed in R. Abbasi et al. (2022a), deliver unbiased parameter estimates for the best-fit number of neutrino events (n_s) and power-law spectral indices (γ), see also Figure 6 (left). We use the same KDE method to derive the PDFs assuming the neutrino fluxes predicted by the disk-corona model. Specifically, we construct these KDEs on a discrete grid as a function of the AGN's intrinsic X-ray luminosity. Assuming the intrinsic X-ray luminosities reported by BASS (C. Ricci et al. 2017), this assigns a unique set of energy and spatial PDFs to each AGN in our selection. Therefore, in contrast to the power-law spectral assumption, there is only a single parameter related to the normalization (the number of signal events n_s). The measurement of this parameter remains unbiased, as demonstrated in Figure 6 (center) for the NGC 1068 as an example. The reduction in variance compared to the power-law case (left) is due to the reduction in degrees of freedom. Assuming the disk-corona model to be correct, we expect the dedicated search to be more powerful than the generic, power-law-based search. Simulations show 10%–20% improvement regarding the signal events needed. Figure 7 shows the increase of the significance using NGC 1068 as an example. We extend the dedicated, model-based search for neutrinos from individual AGN to the stacking case, i.e., the search for combined signals from the set of Seyfert galaxies selected for this work. The

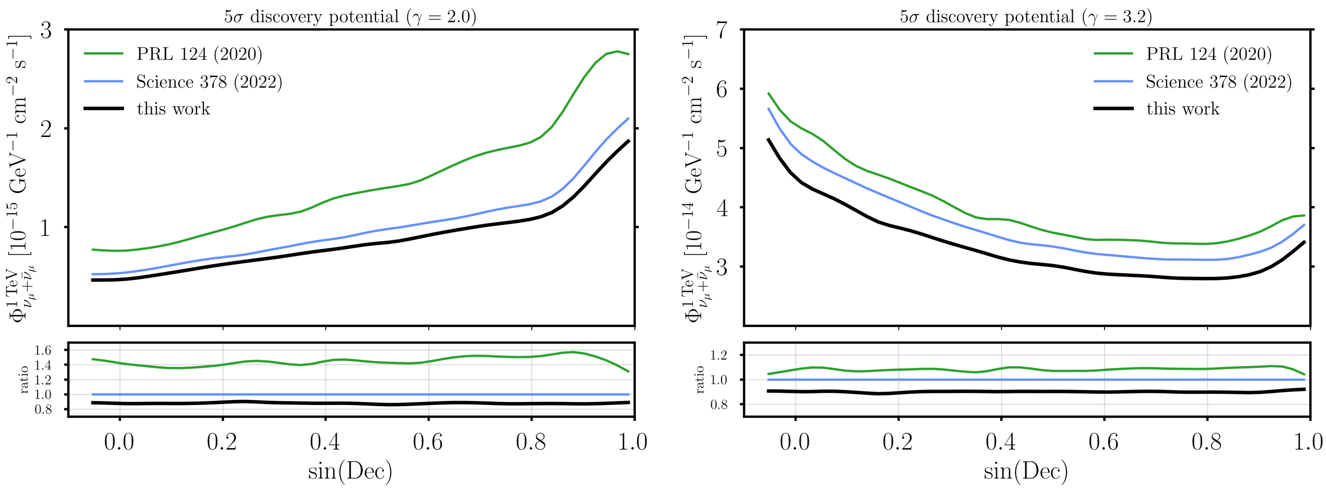

Figure 5. The discovery potential comparison between M. G. Aartsen et al. (2020), R. Abbasi et al. (2022a), and this work for a time-integrated search assuming a power-law spectrum as a function of the source decl. Shown here are the flux levels and the ratios assuming spectral indices $\gamma = 2.0$ (left) and $\gamma = 3.2$ (right).

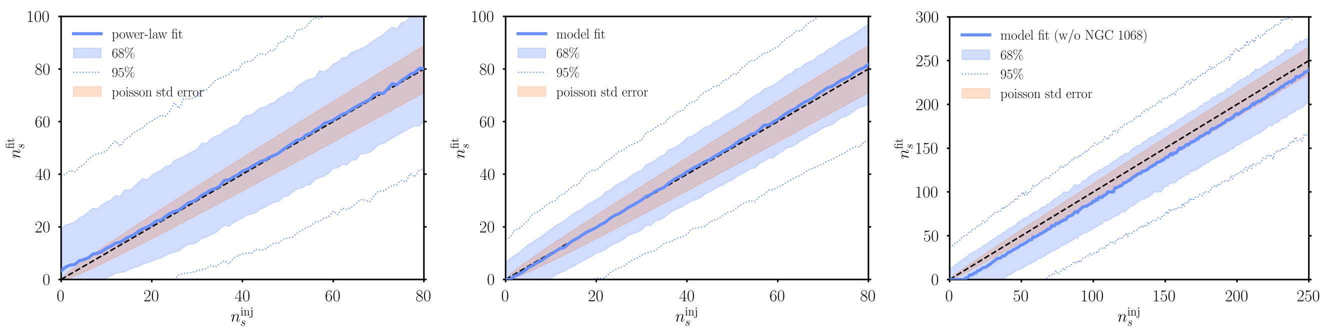

Figure 6. Fitting bias checks. Fitted n_s vs. injected n_s assuming power-law spectrum with $\gamma = 3$ (left) and a spectrum predicted by the disk-corona model (middle) for NGC 1068. Same comparison for the stacking search with the disk-corona model flux assumption (right).

corresponding likelihood function reads

$$L(\mu_s, | \boldsymbol{x}) = \prod_{i=1}^{N} \left\{ \frac{\mu_s}{N} \left[\sum_{k=1}^{N_{src}} w_k f_s(\boldsymbol{x_i} \mid L_k^{2-10\,\mathrm{keV}}, \ \delta_k) \right] + \left(1 - \frac{\mu_s}{N}\right) f_b(\boldsymbol{x_i}) \right\}, \tag{A1}$$

where the relative weights, $0 < w_k < 1$, are given by the number of neutrinos expected from IceCube's effective area and the neutrino flux predicted by the disk-corona model for each source depending on the intrinsic X-ray luminosity

$$w_k = n_k^{exp}(L_k^{2-10\,\mathrm{keV}}, \delta_k) \times \left\{ \sum_k^N n_k^{exp}(L_k^{2-10\,\mathrm{keV}}, \delta_k) \right\}^{-1}. \tag{A2}$$

Recovering some fixed number of signal neutrinos from a set of sources is more challenging than recovering the same number of signal neutrinos from a single source because the effective amount of background is larger. Nevertheless, the estimate of the number of signal events in this analysis also remains essentially unbiased in the stacking case, as shown in Figure 6 (right).

To facilitate an easier comparison to previous works, we have also analyzed our selection of Seyfert galaxies assuming a single power-law flux. The measured flux normalizations and spectral indices for the three most-significant sources (NGC 1068, NGC 4151, and CGCG 420-015) are given in Figure 3. The uncertainties presented here are the statistical ones. The detailed study of systematic uncertainties for this

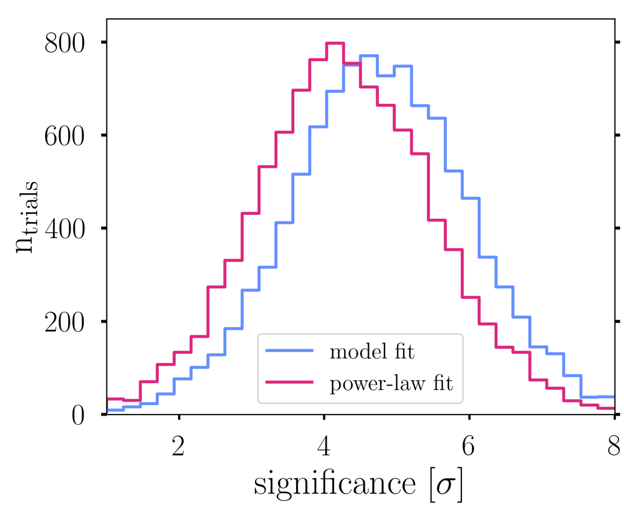

Figure 7. The significance comparison between fitting the model (blue) and power-law (orange) spectra for NGC 1068 when simulating the flux predicted by the disk-corona model. The improvement depends on the source and an increase of 0.7σ is expected for NGC 1068.

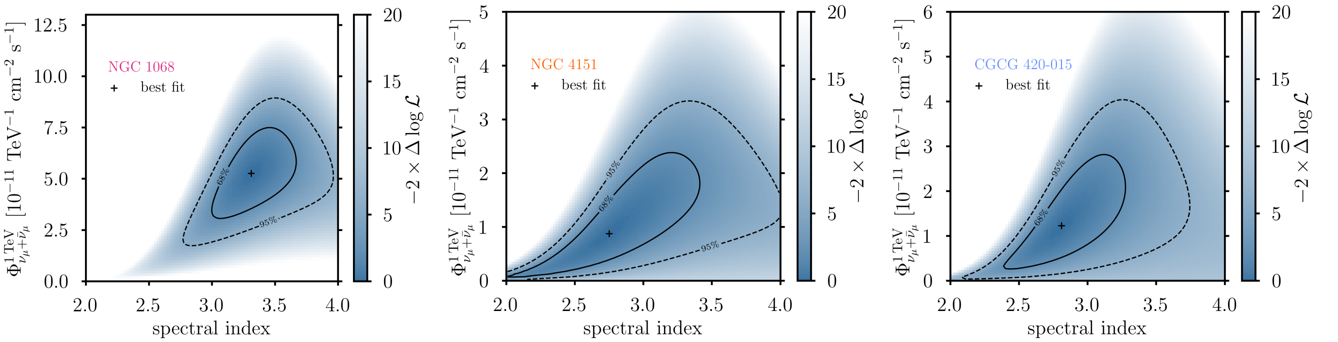

Figure 8. Profile likelihood scans for the flux parameters for the most-significant sources, assuming a power-law spectrum: NGC 1068 (left), NGC 4151 (middle), and CGCG 420-015 (right). The crosses show the best-fit values while contours correspond to the 68% (solid) and 95% (dashed) confidence regions.

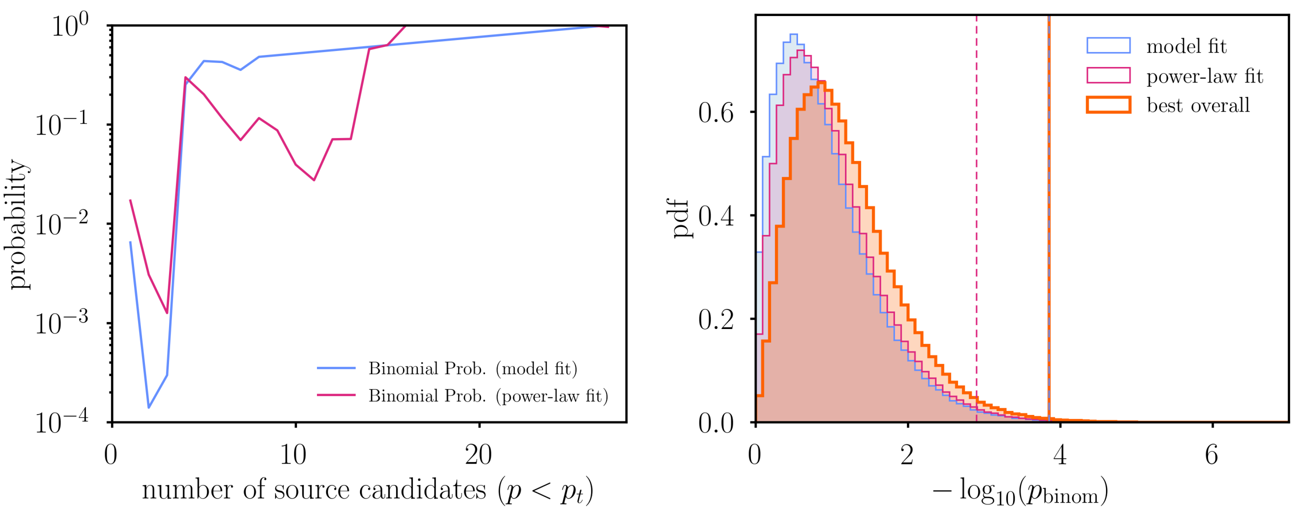

Figure 9. Binomial test for the catalog. Left: Scans of the p-value threshold for the disk-corona model (red) and the power-law spectrum (blue). The strongest excess is found at $k = 2$ (NGC 4151 and CGCG 420-015) assuming the disk-corona model flux. Right: Distributions of binomial p-value in background simulations. The vertical dashed lines denote the observed binomial p-values with the experimental data assuming the power-law flux (red) and disk-corona model flux (blue). The trial-corrected distribution corresponds to the orange histogram and the final p-value is denoted by the orange line.

sample was presented in the supplemental material of R. Abbasi et al. (2022a). These include the depth-dependent optical properties of the glacial ice, the refrozen hole ice columns around the IceCube strings, as well as the photon detection efficiency of the IceCube DOMs. Their effect on the fitted parameters, studied via dedicated MC simulations of alternative detector properties, is subdominant compared to the statistical uncertainties. For NGC 1068, for which statistical uncertainties are smallest, the systematic uncertainties are at the level of ∼10% (∼30%) of the statistical ones for the mean number of signal events (spectral index). Generally, systematic uncertainties yield ±10% uncertainty on the normalization of the neutrino flux (M. G. Aartsen et al. 2019). The neutrino energy range of the best-fitted flux in Figure 3 contains 68% central bins contribution to the total test statistics (TS) value. We calculate the TS contribution for a given neutrino energy bin by creating a histogram of the weighted sum of neutrino energies selected from similar events in MC (having close angular uncertainty and reconstructed energy values), with weights given by each event's contribution to the total TS value. The resulting neutrino energy range depends on the best-fitted flux shape. For the power-law flux, we can see how the larger best-fitted $\hat{\gamma}$ spectral index value results in the lower energy range of NGC 1068 in comparison to energy ranges of NGC 4151 and CGCG 420–015, where the best-fitted $\hat{\gamma}$ spectral indices are lower. The best-fitting values for the entire selection of sources are given in Table 2. The profile likelihood for the powerlaw flux search is shown in Figure 8.

A search for aggregated neutrino signals using the stacking method described above can fail if the model misspecifies individual candidate sources, but is otherwise mostly correct. The binomial test trades a reduction in sensitivity for increased robustness. It simply considers a subset of sources that show positive results in the single source analysis. Here, we perform it twice—one binomial test for each of the two spectral assumptions: disk-corona model and single power law. The test uses the pretrial p-values of the sources to examine an excess in the number of small p-values compared to the expectation from the background. The probability of producing k or more sources with p-values smaller than p_k from background is

$$p_{bkg} = \sum_{i=k}^{N_{src}} \binom{N_{\mathrm{src}}}{i} p_k (1 - p_k)^{N_{src}-i}, \quad \text{(A3)}$$

where we search for the minimum probability $p_{\min}$ and its corresponding k. The expected distribution of $p_{\min}$ for the background used to evaluate the significance is estimated from pseudo-experiments. Figure 9 (left) shows the binomial probability as a function of the number of sources that exceed a given local p-value threshold for the power-law flux (blue) and the disk-corona model flux (red) assumptions. Overall, the smallest binomial probability $p_{\rm min} = 1.4 \times 10^{-4}$ is found for $k = 2$ sources (NGC 4151 and CGCG 420-015) assuming the disk-corona model flux. This does not determine the final significance because we have to account for the internal trials related to the scan over the local p-value thresholds, as well as the choice of two flux models. To determine the final p-value, we perform a large number of repetitions of this search using simulated data that containing only background events. Figure 9 (right) shows the distribution of the best binomial p-value under the power-law spectral and the corona-disk model assumptions. Having scanned the threshold local p-value during the binomial scan increases the p-value from $p_{\rm min} = 1.4 \times 10^{-4}$ to $p_{\rm min}^{\rm corr} = 1.7 \times 10^{-3}$. Selecting the best solution among the two flux assumptions further increases the p-value to $p_{\rm final} = 3.4 \times 10^{-3}$, or 2.7$\sigma$ (orange).

ORCID iDs

R. Abbasi https://orcid.org/0000-0001-6141-4205
M. Ackermann https://orcid.org/0000-0001-8952-588X
S. K. Agarwalla https://orcid.org/0000-0002-9714-8866
J. A. Aguilar https://orcid.org/0000-0003-2252-9514
M. Ahlers https://orcid.org/0000-0003-0709-5631
J. M. Alameddine https://orcid.org/0000-0002-9534-9189
K. Andeen https://orcid.org/0000-0001-9394-0007
C. Argüelles https://orcid.org/0000-0003-4186-4182
S. N. Axani https://orcid.org/0000-0001-8866-3826
X. Bai https://orcid.org/0000-0002-1827-9121
A. Balagopal V. https://orcid.org/0000-0001-5367-8876
S. W. Barwick https://orcid.org/0000-0003-2050-6714
V. Basu https://orcid.org/0000-0002-9528-2009
J. J. Beatty https://orcid.org/0000-0003-0481-4952
J. Becker Tjus https://orcid.org/0000-0002-1748-7367
J. Beise https://orcid.org/0000-0002-7448-4189
C. Bellenghi https://orcid.org/0000-0001-8525-7515
S. BenZvi https://orcid.org/0000-0001-5537-4710
E. Bernardini https://orcid.org/0000-0003-3108-1141
E. Blaufuss https://orcid.org/0000-0001-5450-1757
L. Bloom https://orcid.org/0009-0005-9938-3164
S. Blot https://orcid.org/0000-0003-1089-3001
J. Y. Book Motzkin https://orcid.org/0000-0001-6687-5959
C. Boscolo Meneguolo https://orcid.org/0000-0001-8325-4329
S. Böser https://orcid.org/0000-0002-5918-4890
O. Botner https://orcid.org/0000-0001-8588-7306
J. Böttcher https://orcid.org/0000-0002-3387-4236
B. Brinson https://orcid.org/0000-0001-9128-1159
M. A. Campana https://orcid.org/0000-0003-4162-5739
J. Carpio https://orcid.org/0000-0003-0667-6557
S. Chattopadhyay https://orcid.org/0009-0006-1352-2248
D. Chirkin https://orcid.org/0000-0003-4911-1345
B. A. Clark https://orcid.org/0000-0003-4089-2245
A. Coleman https://orcid.org/0000-0003-1510-1712
J. M. Conrad https://orcid.org/0000-0002-6393-0438
P. Coppin https://orcid.org/0000-0001-6869-1280
P. Correa https://orcid.org/0000-0002-1158-6735
D. F. Cowen https://orcid.org/0000-0003-4738-0787
P. Dave https://orcid.org/0000-0002-3879-5115
C. De Clercq https://orcid.org/0000-0001-5266-7059
J. J. DeLaunay https://orcid.org/0000-0001-5229-1995
D. Delgado https://orcid.org/0000-0002-4306-8828
A. Desai https://orcid.org/0000-0001-7405-9994
P. Desiati https://orcid.org/0000-0001-9768-1858
K. D. de Vries https://orcid.org/0000-0002-9842-4068
G. de Wasseige https://orcid.org/0000-0002-1010-5100
T. DeYoung https://orcid.org/0000-0003-4873-3783
A. Diaz https://orcid.org/0000-0001-7206-8336
J. C. Díaz-Vélez https://orcid.org/0000-0002-0087-0693
H. Dujmovic https://orcid.org/0000-0003-1891-0718
M. A. DuVernois https://orcid.org/0000-0002-2987-9691
P. Eller https://orcid.org/0000-0001-6354-5209
D. Elsässer https://orcid.org/0000-0001-6796-3205
H. Erpenbeck https://orcid.org/0000-0001-6319-2108
A. R. Fazely https://orcid.org/0000-0002-6907-8020
A. Fedynitch https://orcid.org/0000-0003-2837-3477
C. Finley https://orcid.org/0000-0003-3350-390X
L. Fischer https://orcid.org/0000-0002-7645-8048
D. Fox https://orcid.org/0000-0002-3714-672X
A. Franckowiak https://orcid.org/0000-0002-5605-2219
P. Fürst https://orcid.org/0000-0002-7951-8042
J. Gallagher https://orcid.org/0000-0001-8608-0408
E. Ganster https://orcid.org/0000-0003-4393-6944
A. Garcia https://orcid.org/0000-0002-8186-2459
A. Ghadimi https://orcid.org/0000-0002-6350-6485
T. Glauch https://orcid.org/0000-0003-1804-4055
T. Glüsenkamp https://orcid.org/0000-0002-2268-9297
S. J. Gray https://orcid.org/0000-0003-2907-8306
S. Griffin https://orcid.org/0000-0002-0779-9623
S. Griswold https://orcid.org/0000-0002-7321-7513
K. M. Groth https://orcid.org/0000-0002-1581-9049
P. Gutjahr https://orcid.org/0000-0001-7980-7285
C. Haack https://orcid.org/0000-0003-3932-2448
A. Hallgren https://orcid.org/0000-0001-7751-4489
L. Halve https://orcid.org/0000-0003-2237-6714
F. Halzen https://orcid.org/0000-0001-6224-2417
H. Hamdaoui https://orcid.org/0000-0001-5709-2100
A. Haungs https://orcid.org/0000-0002-9638-7574
K. Helbing https://orcid.org/0000-0003-2072-4172
J. Hellrung https://orcid.org/0009-0006-7300-8961
N. Heyer https://orcid.org/0000-0001-9036-8623
C. Hill https://orcid.org/0000-0003-0647-9174
S. Hori https://orcid.org/0009-0007-2644-5955
M. Hostert https://orcid.org/0000-0002-9584-8877
W. Hou https://orcid.org/0000-0003-3422-7185
T. Huber https://orcid.org/0000-0002-6515-1673
K. Hultqvist https://orcid.org/0000-0003-0602-9472
M. Hünnefeld https://orcid.org/0000-0002-2827-6522
W. Iwakiri https://orcid.org/0000-0002-0207-9010
O. Janik https://orcid.org/0009-0007-3121-2486
G. S. Japaridze https://orcid.org/0000-0002-7000-5291
M. Jeong https://orcid.org/0000-0003-2420-6639
M. Jin https://orcid.org/0000-0003-0487-5595
B. J. P. Jones https://orcid.org/0000-0003-3400-8986
D. Kang https://orcid.org/0000-0002-5149-9767
W. Kang https://orcid.org/0000-0003-3980-3778
A. Kappes https://orcid.org/0000-0003-1315-3711
T. Karg https://orcid.org/0000-0003-3251-2126

M. Karl https://orcid.org/0000-0003-2475-8951
A. Karle https://orcid.org/0000-0001-9889-5161
U. Katz https://orcid.org/0000-0002-7063-4418
M. Kauer https://orcid.org/0000-0003-1830-9076
J. L. Kelley https://orcid.org/0000-0002-0846-4542
A. Khatee Zathul https://orcid.org/0000-0002-8735-8579
A. Kheirandish https://orcid.org/0000-0001-7074-0539
J. Kiryluk https://orcid.org/0000-0003-0264-3133
S. R. Klein https://orcid.org/0000-0003-2841-6553
A. Kochocki https://orcid.org/0000-0003-3782-0128
R. Koirala https://orcid.org/0000-0002-7735-7169
H. Kolanoski https://orcid.org/0000-0003-0435-2524
T. Kontrimas https://orcid.org/0000-0001-8585-0933
C. Kopper https://orcid.org/0000-0001-6288-7637
D. J. Koskinen https://orcid.org/0000-0002-0514-5917
P. Koundal https://orcid.org/0000-0002-5917-5230
M. Kovacevich https://orcid.org/0000-0002-5019-5745
M. Kowalski https://orcid.org/0000-0001-8594-8666
K. Kruiswijk https://orcid.org/0009-0002-9261-0537
A. Kumar https://orcid.org/0000-0002-8367-8401
N. Kurahashi https://orcid.org/0000-0003-1047-8094
N. Lad https://orcid.org/0000-0001-9302-5140
C. Lagunas Gualda https://orcid.org/0000-0002-9040-7191
M. Lamoureux https://orcid.org/0000-0002-8860-5826
M. J. Larson https://orcid.org/0000-0002-6996-1155
F. Lauber https://orcid.org/0000-0001-5648-5930
J. P. Lazar https://orcid.org/0000-0003-0928-5025
J. W. Lee https://orcid.org/0000-0001-5681-4941
K. Leonard DeHolton https://orcid.org/0000-0002-8795-0601
A. Leszczyńska https://orcid.org/0000-0003-0935-6313
J. Liao https://orcid.org/0009-0008-8086-586X
M. Lincetto https://orcid.org/0000-0002-1460-3369
Q. R. Liu https://orcid.org/0000-0003-3379-6423
L. Lu https://orcid.org/0000-0003-3175-7770
F. Lucarelli https://orcid.org/0000-0002-9558-8788
W. Luszczak https://orcid.org/0000-0003-3085-0674
Y. Lyu https://orcid.org/0000-0002-2333-4383
J. Madsen https://orcid.org/0000-0003-2415-9959
E. Magnus https://orcid.org/0009-0008-8111-1154
E. Manao https://orcid.org/0009-0002-6197-8574
S. Mancina https://orcid.org/0009-0003-9879-3896
I. C. Mariş https://orcid.org/0000-0002-5771-1124
S. Marka https://orcid.org/0000-0002-3957-1324
Z. Marka https://orcid.org/0000-0003-1306-5260
R. Maruyama https://orcid.org/0000-0003-2794-512X
F. Mayhew https://orcid.org/0000-0001-7609-403X
F. McNally https://orcid.org/0000-0002-0785-2244
K. Meagher https://orcid.org/0000-0003-3967-1533
M. Meier https://orcid.org/0000-0002-9483-9450
L. Merten https://orcid.org/0000-0003-1332-9895
T. Montaruli https://orcid.org/0000-0001-5014-2152
R. W. Moore https://orcid.org/0000-0003-4160-4700
M. Moulai https://orcid.org/0000-0001-7909-5812
T. Mukherjee https://orcid.org/0000-0002-0962-4878
R. Naab https://orcid.org/0000-0003-2512-466X
R. Nagai https://orcid.org/0000-0001-7503-2777
J. Necker https://orcid.org/0000-0003-0280-7484
L. Neste https://orcid.org/0000-0002-4829-3469
H. Niederhausen https://orcid.org/0000-0002-9566-4904
M. U. Nisa https://orcid.org/0000-0002-6859-3944
K. Noda https://orcid.org/0000-0003-1397-6478
A. Obertacke Pollmann https://orcid.org/0000-0002-2492-043X
V. O'Dell https://orcid.org/0000-0003-0903-543X
B. Oeyen https://orcid.org/0000-0003-2940-3164
E. O'Sullivan https://orcid.org/0000-0003-1882-8802
H. Pandya https://orcid.org/0000-0002-6138-4808
N. Park https://orcid.org/0000-0002-4282-736X
E. N. Paudel https://orcid.org/0000-0001-9276-7994
L. Paul https://orcid.org/0000-0003-4007-2829
C. Pérez de los Heros https://orcid.org/0000-0002-2084-5866
S. Philippen https://orcid.org/0000-0002-0276-0092
A. Pizzuto https://orcid.org/0000-0002-8466-8168
M. Plum https://orcid.org/0000-0001-8691-242X
B. Pries https://orcid.org/0000-0003-4811-9863
C. Raab https://orcid.org/0000-0001-9921-2668
A. Rehman https://orcid.org/0000-0001-7616-5790
E. Resconi https://orcid.org/0000-0003-0705-2770
W. Rhode https://orcid.org/0000-0003-2636-5000
B. Riedel https://orcid.org/0000-0002-9524-8943
M. Rongen https://orcid.org/0000-0002-7057-1007
A. Rosted https://orcid.org/0000-0003-2410-400X
C. Rott https://orcid.org/0000-0002-6958-6033
T. Ruhe https://orcid.org/0000-0002-4080-9563
I. Safa https://orcid.org/0000-0001-8737-6825
D. Salazar-Gallegos https://orcid.org/0000-0002-9312-9684
A. Sandrock https://orcid.org/0000-0002-6779-1172
M. Santander https://orcid.org/0000-0001-7297-8217
S. Sarkar https://orcid.org/0000-0002-1206-4330
S. Sarkar https://orcid.org/0000-0002-3542-858X
H. Schieler https://orcid.org/0000-0002-2637-4778
S. Schindler https://orcid.org/0000-0001-5507-8890
F. Schlüter https://orcid.org/0000-0002-5545-4363
J. Schneider https://orcid.org/0000-0001-7752-5700
F. G. Schröder https://orcid.org/0000-0001-8495-7210
L. Schumacher https://orcid.org/0000-0001-8945-6722
S. Sclafani https://orcid.org/0000-0001-9446-1219
M. Seikh https://orcid.org/0000-0002-4464-7354
S. Seunarine https://orcid.org/0000-0003-3272-6896
P. Sevle Myhr https://orcid.org/0009-0005-9103-4410
N. Shimizu https://orcid.org/0000-0001-6857-1772
M. Silva https://orcid.org/0000-0001-6940-8184
B. Skrzypek https://orcid.org/0000-0002-0910-1057
B. Smithers https://orcid.org/0000-0003-1273-985X
D. Soldin https://orcid.org/0000-0003-3005-7879
P. Soldin https://orcid.org/0000-0003-1761-2495
G. Sommani https://orcid.org/0000-0002-0094-826X
G. M. Spiczak https://orcid.org/0000-0002-0030-0519
C. Spiering https://orcid.org/0000-0001-7372-0074
T. Stezelberger https://orcid.org/0000-0003-2676-9574
T. Stuttard https://orcid.org/0000-0001-7944-279X
G. W. Sullivan https://orcid.org/0000-0002-2585-2352
I. Taboada https://orcid.org/0000-0003-3509-3457
S. Ter-Antonyan https://orcid.org/0000-0002-5788-1369
W. G. Thompson https://orcid.org/0000-0003-2988-7998
J. Thwaites https://orcid.org/0000-0001-9179-3760
K. Tollefson https://orcid.org/0000-0001-9725-1479
S. Toscano https://orcid.org/0000-0002-1860-2240
A. Trettin https://orcid.org/0000-0003-0350-3597
M. A. Unland Elorrieta https://orcid.org/0000-0002-6124-3255

A. K. Upadhyay https://orcid.org/0000-0003-1957-2626
N. Valtonen-Mattila https://orcid.org/0000-0002-1830-098X
J. Vandenbroucke https://orcid.org/0000-0002-9867-6548
N. van Eijndhoven https://orcid.org/0000-0001-5558-3328
J. van Santen https://orcid.org/0000-0002-2412-9728
S. Verpoest https://orcid.org/0000-0002-3031-3206
C. Walck https://orcid.org/0000-0002-4188-9219
A. Wang https://orcid.org/0009-0006-9420-2667
C. Weaver https://orcid.org/0000-0003-2385-2559
J. Weldert https://orcid.org/0000-0002-3709-2354
C. Wendt https://orcid.org/0000-0001-8076-8877
N. Whitehorn https://orcid.org/0000-0002-3157-0407
C. H. Wiebusch https://orcid.org/0000-0002-6418-3008
L. Witthaus https://orcid.org/0009-0000-0666-3671
M. Wolf https://orcid.org/0000-0001-9991-3923
S. Yoshida https://orcid.org/0000-0003-2480-5105
S. Yu https://orcid.org/0000-0003-4811-9863
T. Yuan https://orcid.org/0000-0002-7041-5872
Z. Zhang https://orcid.org/0000-0002-7347-283X
P. Zhelnin https://orcid.org/0000-0003-1019-8375

References

Aartsen, M. G., Abbasi, R., Abdou, Y., et al. 2013a, PhRvL, 111, 021103
Aartsen, M. G., Ackermann, M., Adams, J., et al. 2020, PhRvL, 124, 051103
Aartsen, M. G., et al. 2013b, Sci, 342, 1242856
Aartsen, M. G., Ackermann, M., Adams, J., et al. 2017, JINST, 12, P03012
Aartsen, M. G., Ackermann, M., Adamds, J., et al. 2019, EPJC, 79, 234
Aartsen, M. G., Ackermann, M., Adams, J., et al. 2020a, PhRvL, 125, 121104
Aartsen, M. G., Ackermann, M., Adams, J., et al. 2020b, PhRvL, 124, 051103
Aartsen, M. G., Abbasi, R., Ackermann, M., et al. 2021, JPhG, 48, 060501
Abbasi, R., Ackermann, M., Adams, J., et al. 2021, ICRC (Berlin), 37, 1130
Abbasi, R., Ackermann, M., Adams, J., et al. 2022a, Sci, 378, 538
Abbasi, R., Ackermann, M., Adams, J., et al. 2022b, ApJ, 928, 50
Abbasi, R., Ackermann, M., Adams, J., et al. 2022c, PhRvD, 106, 022005
Abbasi, R., Ackermann, M., Adams, J., et al. 2023, Sci, 380, 6652
Abbasi, R., Ackermann, M., Adams, J., et al. 2025, ApJ, 981, 131
Abbasi, R., Ackermann, M., Adams, J., et al. 2024, PhRvD, 110, 022001
Abdollahi, S., Acero, F., Ackermann, M., et al. 2020, ApJS, 247, 33
Acciari, V. A., Ansoldi, S., Antonelli, L. A., et al. 2019, ApJ, 883, 135
Ackermann, M., Ajello, M., Albert, A., et al. 2015, ApJ, 799, 86
Adrian-Martinez, S., Ageron, M., Aharonian, F., et al. 2016, JPhG, 43, 084001
Agostini, M., Böhmer, M., Bosma, J., et al. 2020, NatAs, 4, 913
Ahlers, M., & Halzen, F. 2017, PTEP, 2017, 12A105
Ajello, M., Shaw, M. S., Romani, R. W., et al. 2012, ApJ, 751, 108
Avrorin, A. D., Avrorin, A. V., Aynutdinov, V. M., et al. 2018, in XXth International Seminar on High Energy Physics (QUARKS-2018), Vol. 191, ed. V. E. Volkova et al. (Les Ulis: EDP Sciences), 01006
Ballet, J., Burnett, T. H., Digel, S. W., & Lott, B. 2020, ApJS, 247, 33
Bauer, F. E., Arévalo, P., Walton, D. J., et al. 2015, ApJ, 812, 116
Bechtol, K., Ahlers, M., Di Mauro, M., Ajello, M., & Vandenbroucke, J. 2017, ApJ, 836, 47
Braun, J., Dumm, J., De Palma, F., et al. 2008, APh, 29, 299
Capanema, A., Esmaili, A., & Murase, K. 2020, PhRvD, 101, 103012
Das, A., Zhang, B. T., & Murase, K. 2024, ApJ, 972, 44
Eichmann, B., Oikonomou, F., Salvatore, S., Dettmar, R.-J., & J., B. T. 2022, ApJ, 939, 43
Fang, K., Gallagher, J. S., & Halzen, F. 2022, ApJ, 933, 190
Fiorillo, D. F. G., Comisso, L., Peretti, E., Petropoulou, M., & Sironi, L. 2024, ApJ, 974, 75
Halzen, F., & Kheirandish, A. 2019, FrASS, 6, 32
Halzen, F., & Zas, E. 1997, ApJ, 488, 669
Inoue, S., Cerruti, M., Murase, K., & Liu, R.-Y. 2023, ICRC (Nagoya), 38, 1161
Inoue, Y., Khangulyan, D., & Doi, A. 2020, ApJL, 891, L33
Kheirandish, A., Murase, K., & Kimura, S. S. 2021, ApJ, 922, 45
Marinucci, A., Bianchi, S., Matt, G., et al. 2016, MNRAS, 456, L94
Miller, K., & Stone, J. 2000, ApJ, 534, 398
Murase, K. 2022a, ApJL, 941, L17
Murase, K. 2022b, Sci, 378, 474
Murase, K., Guetta, D., & Ahlers, M. 2016, PhRvL, 116, 071101
Murase, K., Karwin, C. M., Kimura, S. S., Ajello, M., & Buson, S. 2024, ApJL, 961, L34
Murase, K., Kimura, S. S., & Meszaros, P. 2020, PhRvL, 125, 011101
Murase, K., & Stecker, F. W. 2023, in The Encyclopedia of Cosmology. Set 2: Frontiers in Cosmology, ed. F. W. Stecker, Volume 2: Neutrino Physics and Astrophysics (Singapore: World Scientific), 483
Oh, K., Koss, M., Markwardt, C. B., et al. 2018, ApJS, 235, 4
Padovani, P., Resconi, E., Ajello, M., et al. 2024, NatAs, 8, 1077
Ricci, C., Trakhtenbrot, B., Koss, M. J., et al. 2017, ApJS, 233, 17
Senno, N., Mészáros, P., Murase, K., Baerwald, P., & Rees, M. J. 2015, ApJ, 806, 24
Tanimoto, A., Ueda, Y., Odaka, H., Yamada, S., & Ricci, C. 2022, ApJS, 260, 30
Torres-Albà, N., Marchesi, S., Zhao, X., et al. 2023, A&A, 678, A154
Willox, E., HAWC Collaboration, et al. 2022, ATeL, 15765, 1
Ye, Z. P., Hu, F., Tian, W., et al. 2023, NatAs, 7, 1497